Environmental Pollution 306 (2022) 119448

Contents lists available at ScienceDirect

Environmental Pollution

journal homepage: www.elsevier.com/locate/envpol

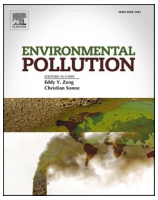

Thallium distribution in an estuary affected by acid mine drainage (AMD): The Ría de Huelva estuary (SW Spain)☆

Carlos Ruiz Cánovas [a], María Dolores Basallote [a,*], Francisco Macías [a], Rémi Freydier [b], Annika Parviainen [c,d], Rafael Pérez-López [a]

[a] Department of Earth Sciences & Research Center on Natural Resources, Health and the Environment. University of Huelva, Campus "El Carmen", E-21071, Huelva, Spain
[b] Laboratoire HydroSciences UMR 5151, CNRS, IRD, Université de Montpellier, 163 Rue Auguste Broussonnet, CC 57, 34090, Montpellier, France
[c] Universidad de Granada, Departamento de Edafología y Química Agrícola, Avda. Fuente Nueva S/n, E-18071, Granada, Spain
[d] Instituto Andaluz de Ciencias de La Tierra (UGR-CSIC), Avda. de Las Palmeras 4, E-18100, Armilla, Granada, Spain

ARTICLE INFO

Keywords:
Schwertmannite
Jarosite
Estuarine mixing processes
Acid mine drainage
Remobilization

ABSTRACT

This study investigates the behavior of Tl in the Ría de Huelva (SW Spain), one of the most metal polluted estuaries in the world. Dissolved Tl concentration displayed a general decrease across the estuary during the dry season (DS); from 5.0 to 0.34 μg/L in the Tinto and Odiel estuaries, respectively, to 0.02 μg/L in the channel where the rivers join. A slighter decrease was observed during the wet season (WS) (from 0.72 to 0.14 μg/L to 0.02 μg/L) due to the dilution effect of rainfalls in the watersheds. These values are 3 orders of magnitude higher than those reported in other estuaries worldwide. Different increases in Tl concentrations with salinity were observed in the upper reaches of the Tinto and Odiel estuaries, attributed to desorption processes from particulate matter. Chemical and mineralogical evidences of particulate matter, point at Fe minerals (*i.e.*, jarosite) as main drivers of Tl particulate transport in the estuary. Unlike other estuaries worldwide, where a fast sorption process onto particulate matter commonly takes place, Tl is mainly desorbed from particulate matter in the Tinto and Odiel estuaries. Thus, Tl may be released back from jarositic particulate matter across the salinity gradient due to the increasing proportion of unreactive $TlCl^0$ and K^+ ions, which compete for adsorption sites with Tl^+ at increasing salinities. A mixing model based on conservative elements revealed a 6-fold increase in Tl concentrations related to desorption processes. However, mining spills like that occurred in May 2017 may contribute to enhance dissolved and particulate Tl concentrations in the estuary as well as to magnify these desorption processes (up to around 1100% of Tl release), highlighting the impact of the mine spill on the remobilization of Tl from the suspended matter to the water column.

1. Introduction

Thallium (Tl) is a non-essential and highly toxic element, considered as a priority pollutant in international regulations (*e.g.*, European Commission, 2000; USEPA, 2015). Thallium may exhibit either lithophile behavior, replacing K^+, Rb^+, and Sr^{2+} in micas and feldspars (Tremel et al., 1997; Law and Turner, 2011) or chalcophile being incorporated as impurity in sulfides (Lis et al., 2003; Liu et al., 2020; Wang et al., 2020; Yin et al., 2021). The weathering of these minerals may lead to increasing levels of Tl in the hydrosphere. Rivers are the main sources of dissolved and particulate metals to the oceans, especially those imbalanced by anthropogenic activities such as mining, which may boost weathering rates and metal transport. For example, the acidic Tinto River (SW Spain) carries annually 0.14 ton of Tl to the Atlantic Ocean (Cánovas et al., 2021). Through the path to the oceans, different geochemical processes may affect Tl mobility. Although Tl exhibits two different oxidation states (*i.e.*, Tl(I) and Tl(III)), Tl(I) prevails in aquatic systems, being Tl^+ the predominant species (Vink, 1993) while Tl(III) may be formed upon strong oxidative processes on oxide surfaces, photoinduced oxidation or bacterial activity (Lin and Nriagu, 1998; Coup and Swedlund, 2015). The solubility of trace cations such as Tl in aquatic systems is commonly limited by sorption to iron oxides.

☆ This paper has been recommended for acceptance by Wen-Xiong Wang.

* Corresponding author.
E-mail address: maria.basallote@dct.uhu.es (M.D. Basallote).

https://doi.org/10.1016/j.envpol.2022.119448
Received 18 February 2022; Received in revised form 28 April 2022; Accepted 6 May 2022
Available online 10 May 2022

Casiot el al. (2011) and Coup and Swedlund (2015) reported that Tl^+ sorption may be only noticeable at alkaline pH values, which explains the high mobility of Tl^+ observed in aquatic environments. Minerals with low zero-point charge (pH_{zpc}) values such as Mn oxides may also play an important role as adsorbent at lower pH values (Belzile and Chen, 2017; Wick et al., 2019). These processes may have a great importance in estuaries where large masses of freshwaters mix with enormous volumes of seawater, leading to intense interaction between suspended particles and the aqueous phase (Turner and Millward, 2002). In this sense, the distribution of Tl in estuaries has been scarcely documented worldwide, and existing literature dealing with Tl partitioning in estuaries (*e.g.*, Nielsen et al., 2005; Turner et al., 2010; Anagboso et al., 2013; Böning et al., 2017) discloses contradictory results. For instance, Nielsen et al. (2005) reported Tl peaks concomitant to maximum values of Mn and Fe due to the remobilization of Fe and Mn-rich suspended particles in two highly turbid zones occurring at low and intermediate salinities in the Amazon estuary. However, more recently, Böning et al. (2017) related the mobility of Tl to the formation of organic complexes in the Weser estuary (Germany), affected by historical sulfide mining. These studies therefore suggest that Tl behavior in estuaries may change depending on several factors such as the riverine dissolved Tl concentration, the abundance and properties of organic matter or the amount and nature of particulate matter within the estuary. In this sense, the Ría de Huelva estuary (SW Spain) is well-known for receiving huge loads of dissolved and particulate metals due to intense mining activity through history (Nieto et al., 2013). Therefore, the main objective of this study is to contribute to fill the gap in knowledge on Tl behavior in estuaries, investigating the mobility of Tl in the Ría de Huelva, one of the most metal polluted estuaries in the world.

2. Methodology

2.1. Site description

The Tinto and Odiel rivers (SW Spain) are heavily polluted by sulfide mining activities developed in their catchments since ancient times. The intense generation of acid mine drainage (AMD) through the years has led to the water quality deterioration of both rivers, with acidic pH values and high metal concentrations (Fig. SM1), becoming a unique case of metal pollution worldwide (Nieto et al., 2013). The confluence of both the acidic Odiel and Tinto rivers (pH 2.5–3.5) with seawater forms an estuarine system known as the Ria de Huelva (Fig. SM1). Inside the estuary, a sharp geochemical gradient is observed, due to the interaction of acidic river waters, which exhibit significant seasonal and annual variations with average daily inflows of 1.6 Mm^3 (Carro et al., 2018), and large volumes of seawater ranging from 37 to 82 Mm^3 during a tidal half-cycle (6 h) (Grande et al., 2000). Thus, the estuary is characterized by two different mixing processes; *i.e.*, a pH-induced mixing process in the upper part, and a salt-induced mixing in the lower one, leading to the progressive precipitation of some metals such as Fe and Al and subsequent deposition in the estuarine sediments (Carro et al., 2018). However, the most mobile metals (*e.g.*, Zn, Cu and Cd) may pass through the estuary giving rise to a metal-rich plume in the coastal waters of the Gulf of Cádiz (*e.g.*, Elbaz-Poulichet et al., 2001) and increasing metal exposure to living organisms (*e.g.*, Cánovas et al., 2020a, 2020b).

2.2. Sampling

Different transects (Fig. SM1) were conducted in the Ría de Huelva estuary following the salinity gradient upon different hydrological regimes (wet season (WS): March 2018; dry season (DS): May 2018). In addition, a sampling along the Odiel River estuary was performed in May 2017, coinciding with the arrival of a mine spill (MS) in the Odiel River (Olías et al., 2019). Both DS and WS samplings were performed during the rising tide to reach the shallowest sections of the estuary (close to the river confluence), with a tidal range of around 2 m and a high tidal coefficient (76–82). In the case of the MS sampling along the Odiel estuary, lower tidal coefficients were recorded (62–66). River contribution varied notably between both samplings, with a noticeable lower contribution during the DS (2.7 m^3/s; 1.4 m^3/s for the Odiel River and 1.3 m^3/s for the Tinto) than during the WS (32.1 m^3/s; 13.5 m^3/s for the Odiel and 18.6 m^3/s for the Tinto). In the case of the MS sampling along the Odiel estuary, it also took place upon low flow conditions (<0.2 m^3/s). Estuarine water samples were taken with a 2 L Niskin bottle at 2 m depth from the surface, to avoid contamination from the ship. In addition, river and seawater samples were also collected during the sampling campaigns to ascertain the influence of each end-member on estuarine waters during mixing processes. Aliquot samples, unfiltered and filtered through 0.22 μm pore size Millipore filters, were stored in high-density polyethylene (HDPE) bottles, and acidified to pH < 2 with nitric acid 65% Merck Suprapur®, and kept refrigerated until analysis. Additionally, aliquots of the filtered samples were kept non-acidified for anion determinations. Particulate metal concentrations were determined by subtracting the concentrations analyzed in the filtered and unfiltered acidified aliquots. In addition, particulate matter was recovered after filtering a great volume (2–5 L) of waters during the May 2018 sampling for chemical and mineralogical characterization. Around 20 mg of these solids were accurately weighed and placed in 15 mL Savillex Teflon vials, and initially digested at room temperature for 24 h with 2 mL of *aqua regia* (3:1; 12 M HCl and 17 M HNO_3). Then, the suspension was digested on hotplate at 130 °C for 3 h. The obtained suspension was cooled until room temperature and evaporated to dryness at 55 °C. Finally, samples were recovered with ultrapure HNO_3 and stored until analysis. All the bottles used were previously acid-washed (10% HCl) for 24 h, rinsed in Milli-Q water (18.2 MΩ·cm, Millipore) and stored in sterile plastic bags.

2.3. Analytical determinations

Different physico-chemical parameters such as temperature, pH, electrical conductivity (EC), and oxidation-reduction potential (ORP) were measured in situ along the estuary using HANNA HI 98190 and 98,192 portable meters. Two different sets of portable meters were used for the river and sea domains to avoid probe instabilities due to the strong gradient of pH and salinity observed. On the one hand, calibration was performed for both EC (147 μS/cm, 1413 μS/cm, 12.88 mS/cm, and 111 mS/cm) and pH (4.01, 7.00, and 9.21), depending on the seawater influence of samples. On the other hand, the ORP was controlled using two different certified materials (240 and 470 mV). Major elements concentrations (Ca, Na, Mg, Al and K) were determined by Inductively Coupled Plasma-Atomic Emission Spectroscopy (ICP-AES; PerkinElmer® Optima 3200 RL) for major elements at the University of Huelva. Trace metal determination in the water samples was performed without any prior dilution using Kinetic energy Discrimination - Argon Gas Dilution (KED-AGD mode) with the Thermo Scientific iCAP TQ ICP-MS (Plateforme AETE-ISO – HydroSciences/OSU OREME, Montpellier – France). An internal solution, containing Be, Sc, Ge, Rh and Ir was added on-line to the samples to correct signal drifts. Estuarine water reference material for trace metals (SLEW-3) was also analyzed to check the analytical accuracy, with all values below 10% of difference with respect to certified values (Table SM1). The relative standard deviation (RSD) values of analysis ranged from 0.1% to 7.2% for all elements. The detection limits for Li, Fe, Mn and Tl were of 0.72 μg/L, 0.11 μg/L, 0.02 μg/L and 0.4 ng/L. In addition, the SO_4^{2-}, Cl^-, F-, and Br^- concentrations were determined using ion chromatography (Dionex DX-120) at the R + D laboratories of the University of Huelva (detection limits of 0.1 mg/L), and the determination of the total alkalinity by CHEMetrics® Total Titrets®, with a range of 10–100 or 100–1000 mg/L as $CaCO_3$ equivalents. The trace element concentrations of the suspended particulate matter collected along the estuary were analyzed by ICP-MS (Agilent 8800 TripleQuad) at the Instituto Andaluz de Ciencias

de la Tierra (IACT, CSIC-UGR, Granada, Spain). The solid samples were also analyzed by bulk powder X-ray diffraction (XRD) using PANAlytical X'PERT PRO diffractometer at IACT. The diffractometer is equipped with an X'Celerator detector and a theta-theta goniometer, and the measurements were performed on the scan range from 3.0 to 70.0 (2θ) with a step size of 0.0167°. The identification of the mineral phases was performed using XPowder software (Martín-Ramos, 2004). Samples were also examined by FEI QemScan 650 F high-resolution Field Emission Environmental Scanning Electron Microscope (SEM) at Centro de Instrumentación Científica (CIC) at Universidad de Granada. The samples were mounted on carbon tape, carbon coated, and back-scattered mode was used for high-resolution imaging of the particles and the semiquantitative chemical composition was examined by energy-dispersive X-ray microanalysis (EDX). The acceleration voltage was set to 20 kV for the data acquisition.

2.4. Data treatment

Chemical speciation of elements was determined by the PHREEQC code v.3.4 (Parkhurst and Appelo, 2013) using the Minteq. v4. dat database (Allison et al., 1999) enlarged with thermodynamic data from Yu et al. (1999) for the solubility of schwertmannite. This database relies on extended Debye-Hückel equations and provides accurate activity calculations in chloride dominated solutions with ionic strengths below 1 mol/L. The ORP measurements were corrected to the standard hydrogen electrode to determine Eh values (Nordstrom and Wilde, 1998). The balance error obtained by the PHREEQC code was below 10% for all the samples. For consistency, the PHREEQC outputs were compared with the chemical speciation obtained using the CHEAQS program version 2017.3 (Verweij, 2017). The CHEAQS model includes inorganic speciation and the mineral equilibrium based on the National Institute of Standards and Technology database version 8.0 (NIST, 2004). Similar speciation results were obtained from both codes.

In order to quantify the river and seawater contribution to the estuarine samples, the code MIX (Carrera et al., 2004) was used. MIX is a maximum likelihood method to estimate mixing ratios, while acknowledging uncertainty in end-member concentrations. The variables to be included in the model need satisfying some conditions to be suitable in mixing models: exhibit a conservative behavior and their values must be significantly different in the extreme components. Thus, the following variables were chosen as end-members: EC, Cl, Na, Br, and Li.

3. Results and discussion

3.1. Dissolved and particulate concentrations

Table 1 shows the basic statistics of obtained results divided into different zones: Tinto estuary, Odiel estuary and main channel. As a consequence of mixing processes of acidic river waters with alkaline seawaters, pH values increased progressively within both estuaries (Fig. 1). For the Tinto estuary, pH ranged from 2.77 to 7.62 during the DS and from 3.89 to 6.32 during the WS. In the case of the Odiel estuary, pH values ranged from 3.95 to 7.99 during the DS and from 4.66 to 7.12

Table 1
Statistics of main physico-chemical parameters dissolved and particulate metal concentrations measured in the Tinto-Odiel estuary during the study period.

						Dissolved						Particulate			
		Temperature (°C)	pH	EC (mS/cm)	ORP (mV)	Cl (mg/L)	Na (mg/L)	Fe (μg/L)	Mn (μg/L)	Al (μg/L)	Tl (μg/L)	Fe (μg/L)	Mn (μg/L)	Al (μg/L)	Tl (μg/L)
Wet season (WS)															
Tinto	N	10	10	10	10	10	10	10	10	9	10	9	9	10	8
	Minimum	12.5	3.6	0.6	167	39	26	30	363	934	0.2	1730	2.4	2.0	b.d.l
	Maximum	19.0	6.3	32	469	14,469	6427	6223	1071	10,336	0.7	11,349	147	31,948	0.1
	Average	13.6	4.5	9.2	349	3468	1515	2087	806	6604	0.6	6578	85	4226	0.1
Odiel	N	8	8	8	8	8	8	8	8	7	8	8	7	8	8
	Minimum	14.3	4.7	0.5	198	42	21	9.3	364	8.2	0.1	244	15	157	b.d.l
	Maximum	15.9	7.1	39	330	15,299	6100	1107	1188	6681	0.1	3694	210	1241	0.0
	Average	15.0	5.7	15.3	370	5562	2413	590	864	3088	0.1	1363	84	761	0.0
Channel	N	7	7	7	7	7	7	7	7	2	7	7	3	6	7
	Minimum	13.7	7.0	43	161	15,397	6807	3.4	23	b.d.l	0.0	337	b.d.l	258	b.d.l
	Maximum	14.9	8.1	56	292	22,354	9154	17	311	154	0.1	718	3.3	507	0.0
	Average	14.2	7.6	47	257	18,502	7789	8.4	180	120	0.1	512	1.9	388	0.0
Dry Season (DS)															
Tinto	N	11	11	11	11	11	11	11	11	10	11	11	11	b.d.l	7
	Minimum	21.2	2.8	2.2	164	277	120	4.6	115	79	0.2	349	29		b.d.l
	Maximum	22.4	7.6	57	516	21,815	9810	62,999	9419	44,207	5.0	4172	940		1.4
	Average	21.9	4.2	25	415	8655	3955	21,293	4639	23,570	2.5	1588	333		0.4
Odiel	N	8	8	8	8	8	8	8	8	8	8	8	8	b.d.l	4
	Minimum	20.9	3.9	8.6	169	2266	1110	3.3	121	253	0.2	44	21		b.d.l
	Maximum	22.0	7.6	57	421	21,554	10,592	1586	8853	31,128	0.34	599	2518		0.3
	Average	21.7	4.0	20	427	6967	3190	379	4894	9681	0.3	1151	293		0.1
Channel	N	7	7	7	7	7	7	7	7	7	7	7	7	b.d.l	b.d.l
	Minimum	19.4	7.7	58	151	21,464	10,444	2.4	5.9	90	0.0	26	0.6		
	Maximum	21.3	8.0	60	186	22,750	11,035	6.5	78	379	0.2	625	22		
	Average	20.2	7.8	59	170	22,136	10,816	4.2	28	188	0.1	206	9.4		
Mine spill (MS)															
Odiel	N	8	8	8	8	8	8	8	8	8	8	8	8	8	b.d.l
	Minimum	22.3	3.1	14	190	6449	3025	5	105	1.0	0.2	97	1.0	150	
	Maximum	23.1	7.4	31	506	19,808	6871	14,970	9822	37,933	0.5	1638	288	2096	
	Average	22.7	5.5	25	312	14,924	5412	3275	3324	10,552	0.4	658	37	658	
Channel	N	7	7	7	7	7	7	7	7	7	7	7	7	6	b.d.l
	Minimum	21.7	7.5	31	153	19,356	6644	4.5	9.2	1.0	0.0	353	6.8	283	
	Maximum	23.2	8.0	46	206	20,574	7189	32	105	362	0.2	1328	26	875	
	Average	22.4	7.8	34	176	20,090	6950	11	29	128	0.1	738	15	550	

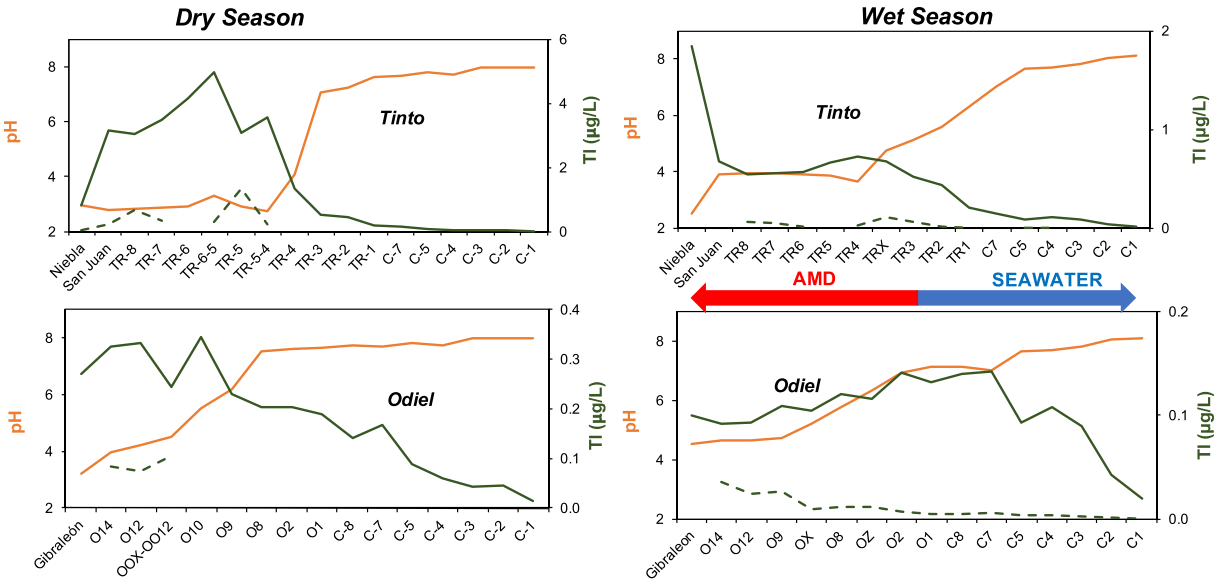

Fig. 1. Evolution of pH and dissolved (solid line) and particulate (dashed line) Tl concentrations in the Tinto and Odiel estuaries, and the common channel during the wet season (WS) and dry season (DS). (AMD = acid mine drainage). Niebla and Gibraleón sampling points are outside the tidal influence.

during the WS. Higher pH values were observed in the common channel, with pH values ranging from 7.0 to 8.1 during the WS and 7.7 and 8.0 during the DS (Table 1). It is striking the narrower pH range observed during the WS, associated with the lower acidity but higher discharge of the Tinto and Odiel rivers during the wet season (Cánovas et al., 2007). In turn, the high acidity but low discharges during the DS led to lower pH values in the upper reaches of both estuaries and higher pH values in the lower ones (Fig. 1) due to intense acidity neutralization. Lower pH values were found across the Tinto estuary due to the higher acidity of the Tinto River waters compared to those of the Odiel River (Nieto et al., 2013). The progressive increase of pH values, together with the dilution effect by seawater, caused a general decrease in metal concentrations within both estuaries. For example, during the WS a decrease from few mg/L of Fe, Al and Mn (up to 6.2 and 1.1 mg/L of Fe, 10 and 6.7 mg/L of Al, and 1.1 and 1.2 mg/L of Mn, in the upper reaches of the Tinto and Odiel estuaries, respectively; Table 1) to few µg/L (8.4 µg/L of Fe, 120 µg/L of Al, and 180 µg/L of Mn) in the lower part (common channel) was observed (Table 1 and Fig. SM1). This decrease in concentrations was noticeably more intense during the dry season; from 63 to 1.6 mg/L of Fe, 44 and 31 mg/L of Al, and 9.4 and 8.8 mg/L of Mn, in the upper reaches of the Tinto and Odiel estuaries, respectively (Table 1), to 2.4 µg/L of Fe, 90 µg/L of Al, and 5.9 µg/L of Mn in the channel. Concerning particulate concentrations, high metal concentrations were observed during the WS in the estuary; maximum values of 11,349 and 3649 mg/L of Fe, 31,948 and 1241 mg/L of Al, or 147 and 210 mg/L of Mn (Table 1) in the upper reaches of the Tinto and Odiel estuaries, respectively. Conversely, significantly lower particulate concentrations were observed during the DS due to the decreased load of suspended particulate matter delivered by the Tinto and Odiel rivers during this period. A similar behavior was observed in the common channel (i.e., higher particulate concentrations during WS), with the exception of Mn, with higher average concentrations during the DS.

Regarding dissolved Tl, its concentration also displayed a decrease across the estuary; from 5.0 to 0.34 µg/L in the Tinto and Odiel estuaries, respectively, to 0.02 µg/L at the end of the common channel during the DS (Table 1). This decrease appears to be more attenuated during the WS due to the dilution effect of rainfalls in the river watersheds; from 0.72 to 0.14 µg/L in the Tinto and Odiel estuaries, respectively, to 0.02 µg/L at the end of the common channel (Table 1). These concentrations are remarkably higher than those reported for other estuaries worldwide, such as the Amazon estuary (0.005–0.017 µg/L; Nielsen et al., 2005); Weser estuary (0.014–0.026 µg/L; Böning et al., 2017), Tamar estuary (0.002–0.010 µg/L; Anagboso et al., 2013). These values even exceed in some cases the threshold limits (0.24–0.47 µg/L) established for priority toxic pollutants by USEPA for human health (USEPA, 2014). However, different studies dealing with human health effects after Tl chronic ingestion provide contradictory results. For instance, Nuvolone et al. (2021) studied the effect of high Tl concentrations (above EPA recommended reference values) in the drinking water distribution of Tuscany (Italy) and they did not report any excess of risk in terms of mortality and hospitalization in the population exposed to Tl compared to those non-exposed from other not contaminated areas. On the other hand, Campanella et al. (2019) reviewed the toxicity of Tl at low doses and highlight that Tl exposure, even at very low concentrations, represents a threat to human health, recommending to revise the concentration limits of Tl in the various environmental compartments.

Fig. 1 displays in detail the evolution of dissolved and particulate concentrations of Tl across the estuary. Different patterns are observed in the Tinto and Odiel estuaries; whereas increasing dissolved Tl concentrations during the DS and decreasing ones during the WS are observed in the upper reach of the Tinto estuary, the opposite trend is observed in the Odiel estuary. In the common channel a clear decrease in concentration is observed in both periods, probably associated to dilution by seawater. Regarding particulate Tl concentrations, this element followed a different behavior than the rest of metals (*e.g.*, Fe, Al and Mn) with higher concentrations observed during the DS (0.45 and 0.10 mg/L in the Tinto and Odiel estuaries, respectively) than in the WS (0.05 and 0.01 mg/L, respectively; Fig. 1 and Table 1). However, particulate concentrations of Tl were negligible for a high number of analyzed samples, where Tl concentrations in filtered and unfiltered samples were similar.

A clearer information is obtained if dissolved Tl concentration is compared to salinity. It is generally expected that during estuarine mixing processes dissolved Tl concentrations may decrease as long as the Cl concentrations increase. Fig. 2 exhibits the relationship between both elements during the WS and DS. As can be seen, a good negative correlation ($R^2 = 0.96$) is observed between Tl and Cl concentrations in the Tinto estuary during the WS, while a poorer one ($R^2 = 0.55$) is observed during the DS, due to the sharp increase in Tl concentration observed in the low salinity zone (<5000 mg/L of Cl; Fig. 2). This increase is also observed during the WS, but of lower magnitude.

In the case of the Odiel estuary, a good positive correlation is

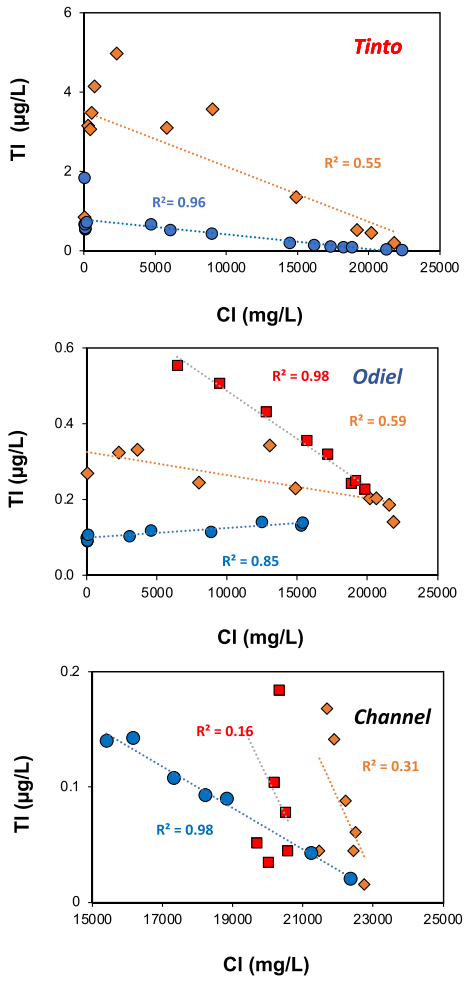

Fig. 2. Relationship between dissolved Tl and Cl concentrations in the different estuarine domains of the Ría de Huelva. Dry season: orange diamonds; Wet season: blue circles; and Odiel Mine spill: red squares. (For interpretation of the references to colour in this figure legend, the reader is referred to the Web version of this article.)

observed during the WS ($R^2 = 0.85$); *i.e.*, the concentration of dissolved Tl increases with salinity, while a poorer one ($R^2 = 0.59$) is observed during the DS, due to an apparent zig-zag evolution (Fig. 2). It also remarkable the good negative correlation ($R^2 = 0.98$) found between Tl and Cl concentrations in the common channel during the WS compared to that observed in the DS. Whereas the concentration of Tl in the channel is still high in the WS due to the higher river contribution, decreasing downward with salinity, the concentration of Tl is quite low in the channel during the DS due to the higher seawater influence, as evidenced by the slight variations of salinity.

3.2. Tl occurrence in the suspended particulate matter of estuarine waters

Suspended particles may play a major role in metal partitioning in estuaries associated to changes in particle concentration and nature, which may control its reactivity, as well as the sharp changes in salinity, pH, redox and concentration of inorganic and organic compounds (Ridderinkhof et al., 2000; Turner and Millward, 2002). Among these factors, the composition and concentration of suspended particles and water salinity may control the partitioning of trace metals in estuarine waters (Turner, 1996). XRD analysis on suspended particulate matter along the estuary revealed the presence of quartz in all samples together with the occurrence of phyllosilicates, however it failed to detect other minor phases due to their poorly-crystalline nature or its concentrations was below 5%, the detection limit of this technique. In this sense, a detailed examination of suspended particulate matter by SEM-EDX (Fig. 3) revealed the presence of Fe oxy (hydr)oxysulfate phases in the Tinto estuary within the pH range from 2.76 to 7.62. These precipitates showed different morphologies with grains of 1–2 µm in diameter with irregular or rounded shape were observed in the upper reach of the estuary (pH < 3), whereas nano-sized acicular shapes were mainly observed in the lower reaches (pH > 3). In the case of the Odiel estuary, the mineral assemblage of suspended particulate matter was dominated by nano-sized globular Al hydroxide, which covered the surfaces of other minerals, including Fe (hydr)oxysulfate.

Saturation indices provided by PHREEQC support the mineralogical evidences observed by SEM-EDS. As can be seen in Fig. SM2, there exists oversaturation of Tinto estuarine waters with respect to different Fe hydroxysulfates such as jarosite and schwertmannite during both periods. Only samples highly influenced by the river (i.e., San Juan) and seawater (i.e., C2 and C1) showed undersaturation with respect to schwertmannite. On the other hand, these waters also exhibited undersaturation with respect $Fe(OH)_3$ and Al mineral phases (*i.e.*, basaluminite and $Al(OH)_3$; Fig. SM3) except at the lower part of the estuary during the wet season. In the case of the Odiel estuarine waters, there exists oversaturation with respect to jarosite, schwertmannite, basaluminite and $Fe(OH)_3$; Fig. SM2), especially in the lower reach of the estuary for this latter mineral. Despite the apparent oversaturation of estuarine waters with respect to jarosite, schwertmannite appears to be the main Fe mineral formed within the estuary as a result of the neutralization of acidic river waters with seawater (Asta et al., 2015; Lecomte et al., 2017) while jarosite may be predominantly transported from the rivers to the estuary. These mineral phases commonly have a great scavenging potential for trace metals such as As, Pb or Tl. For instance, schwertmannite may retain significant amounts of trace metal/loids such as Al, Cu, As or Pb (Acero et al., 2006) whereas jarosite may scavenge Tl by both K^+ and Fe(III) substitution (*e.g.*, Dutrizac et al., 2005; Aguilar-Carrillo et al., 2020). A comparison between the components of the suspended particulate matter collected along the estuary could provide a hint about the origin of Tl in this matter transported along the estuary. Fig. 4 shows the relationship between the concentration of Tl and other elements in the suspended particulate matter collected during the May 2018 (DS) sampling in both estuaries. As can be seen, Tl exhibits a good positive linear correlation with Fe ($R^2 = 0.86$) and negative with Al ($R^2 = 0.87$), which points out at Fe minerals as main Tl carrier phases in the estuary and suggest the existence of two different alternating domains of metal transport, a Fe-dominating and Al-dominating particulate transport. This fact supports the recent finding of Cánovas et al. (2021), according to which a high correlation of Tl with Fe in suspended particulate matter transported by the Tinto River is observed due to its incorporation into jarosite. These authors also found a high correlation of Tl with Si (and not with Al), attributed to the incorporation of Tl in the siliceous frustules of diatoms or the coating of jarosite onto clay particles. Jacobson et al. (2005) suggest that Tl may incorporate into the interlayers of illitic and vermiculitic clays. However, no correlation was observed between Si and Tl (Fig. 4) in the suspended particulate matter. Although Tl may be adsorbed onto Mn oxides (Wick et al., 2019), there was no correlation between these elements either, suggesting that particulate Tl transport in the estuary is exclusively driven by Fe minerals.

In addition to Tl, Fe mineral phases can also host significant concentrations of other trace metals. For example, there exists a high correlation between Tl and As ($R^2 = 0.81$), a metalloid commonly scavenged during Fe minerals precipitation. To a lesser extent, P also showed a good correlation with Tl, since P is also intensively incorporated into Fe minerals (Sibrell et al., 2009). However, other element such as Pb that also regularly incorporates into these minerals did not exhibit good correlations with Tl. Moreover, Tl^+ can also replace Rb^+ and K^+ in micas and feldspars transported by the river, however, only a moderate correlation was observed between Tl and Rb ($R^2 = 0.59$),

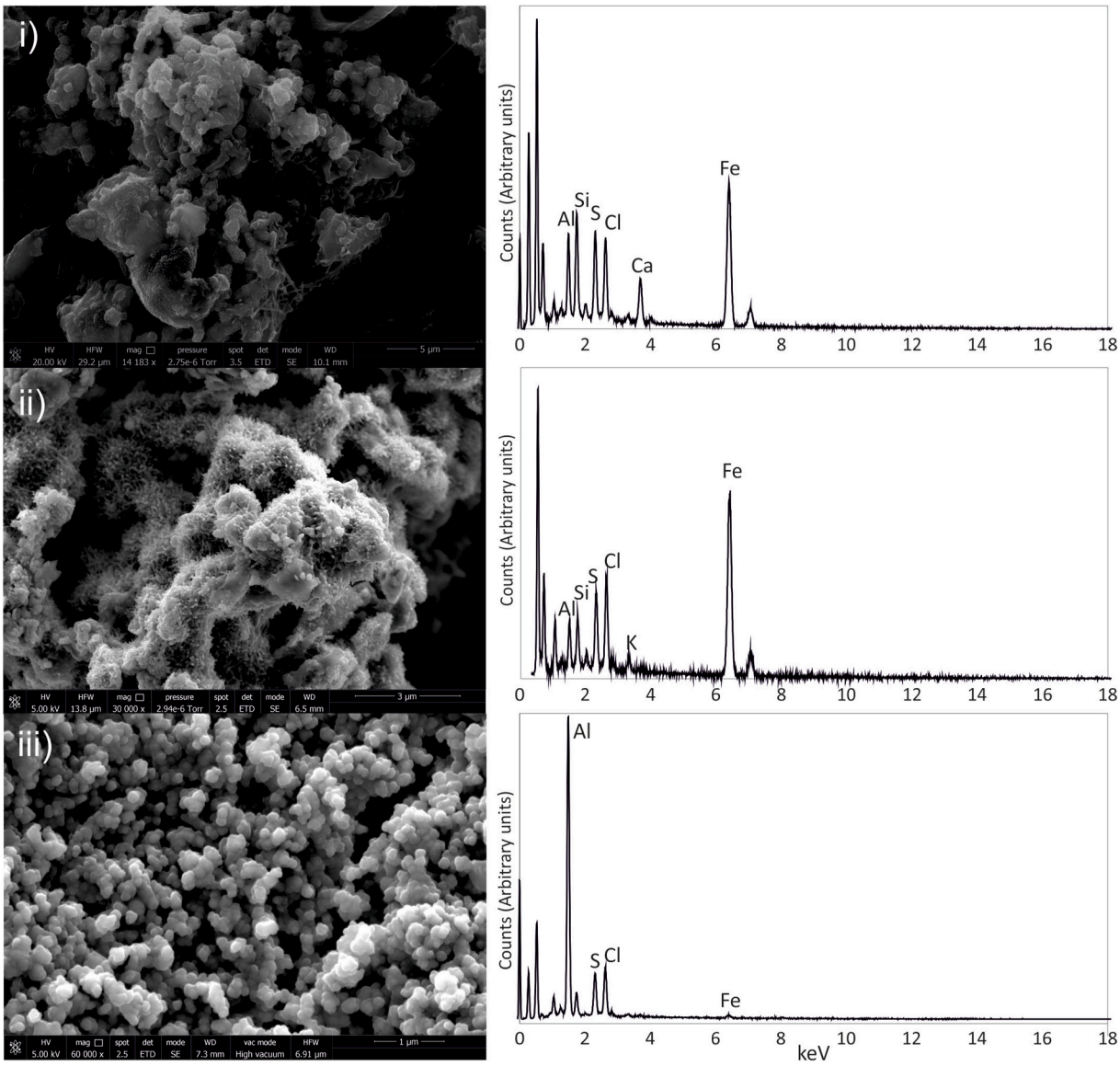

Fig. 3. SEM-EDS images of minerals identified in the suspended particulate matter collected along the estuary. From top to bottom; i) Fe (hydr)oxysulfate grains of 1–2 μm with irregular or rounded shape in the Tinto estuary, ii) Fe (hydr)oxysulfate grains of acicular shape in the Tinto estuary and iii) rounded/globular grains of Al (hydr)oxides in the Odiel estuary.

whereas a poor negative correlation was observed for K ($R^2 = 0.29$). Therefore, no solid relationships between Tl and these elements could be established.

3.3. The role of particle-water interactions in the mobility of Tl

Interactions between suspended particles and the water column may result from different physical, chemical and biological processes such as precipitation/dissolution, colloid aggregation, ion exchange, adsorption-desorption, etc. (Turner and Millward, 2002). The increase in Tl concentration with salinity observed in the estuary, especially in the low salinity zone (Fig. 2) could be related to suspended particle-water interactions. A hypothesis could be the desorption of Tl^+ from the jarosite structure during the mixing of river with seawater. Competitive sorption between Tl^+ and K^+ for incorporation into the structural sites in jarosite structure has been previously reported at laboratory and field conditions (Aguilar-Carrillo et al., 2020). During estuarine mixing processes competitive adsorption by seawater cations may take place, as well as the formation of stable complexes with sulfate, chloride or carbonate (Webster et al., 1995). Turner et al. (2010) reported that Tl adsorption may decrease across the salinity gradient owing to the reduction in the concentration and activity of Tl^+, and an increasing proportion of unreactive $TlCl^0$ and K^+ ions, which compete for adsorption sites with Tl^+ at increasing salinity. Fig. SM4 and Tables SM2-SM4 shows the Tl speciation distribution across the salinity gradient. As can be seen, Tl^+ is the dominant species when pH values remain below 4 in both estuaries during the DS, with values ranging from 45 to 90% of total Tl. This predominance of Tl^+ is greater in both estuaries during the WS due to the higher contribution of river waters. The abundance of $TlCl^0$ increases across the salinity gradient, from values of 2% to around 45% of total Tl in both estuaries during the DS, being slightly lower during the WS (Fig. SM4).

Although previous studies reported that Tl is adsorbed on estuarine suspended particles in a very fast process (Turner et al., 2010), the suspended particulate matter composition (Fig. 4) and Tl speciation (Fig. SM4), suggest that the opposite process is taking place. Thus, the Tl^+ incorporated into the structure of jarosite carried mainly by the rivers may be desorbed or released as a consequence of cation exchange

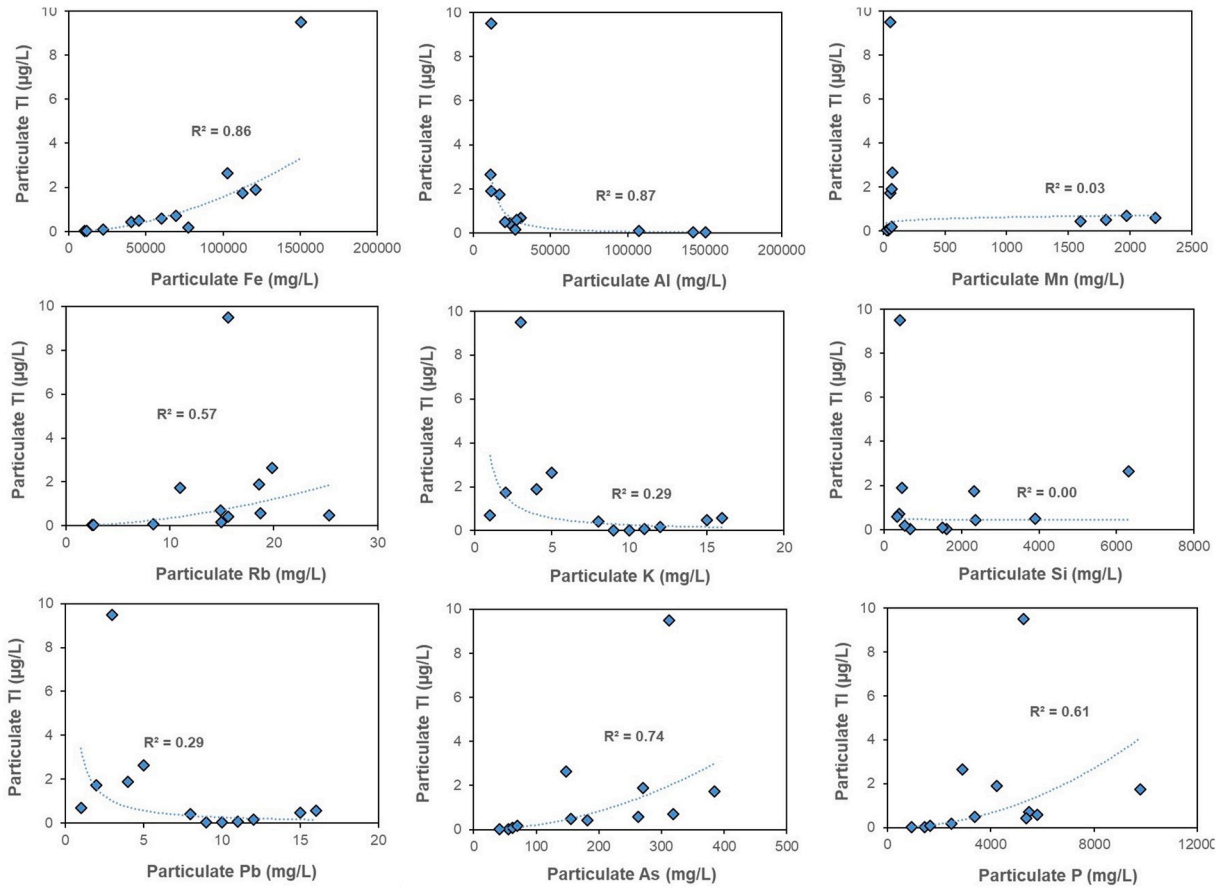

Fig. 4. Relationship between the concentration of Tl and other elements in the suspended particulate matter collected along the estuary.

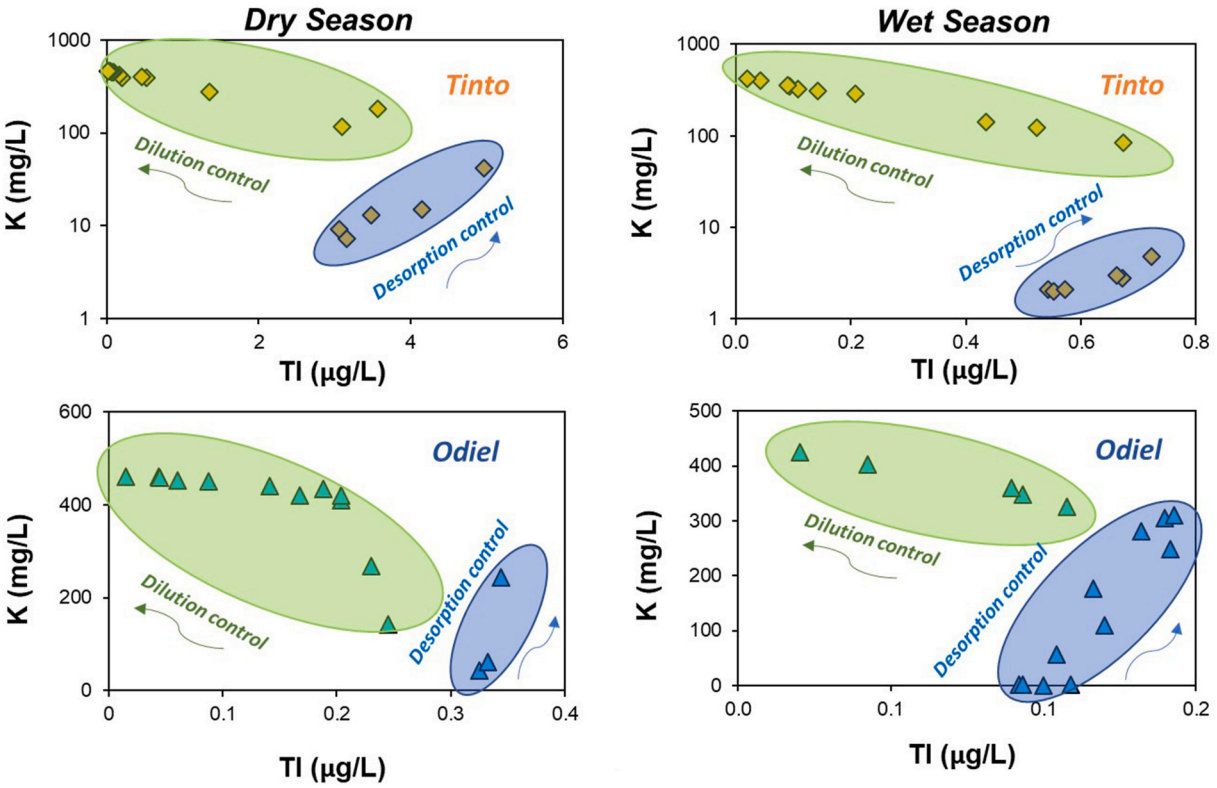

Fig. 5. Comparison of the dissolved concentrations of K and Tl in estuarine waters during both the dry and wet seasons (see text for explanation).

processes with K^+ as salinity increases. As can be seen in Fig. 5, where the concentrations of dissolved Tl are represented versus those of K, an initial increase in Tl concentrations is observed in the upper part of both estuaries when K concentration rises. In this estuarine zone, the concentration of dissolved Tl would be controlled by desorption processes from jarosite minerals. Once the seawater influence is higher, with increasing concentrations of K^+, Tl is mainly complexed by Cl, remaining in solution, and its concentration may be mainly controlled by dilution processes (Fig. 5).

3.4. Conservative/non-conservative behavior of Tl in the estuary

In order to study the contribution of both end-members (*i.e.*, acidic river water and seawater) and the behavior of Tl during the estuarine mixing processes, a mixing model was performed using the MIX code. The goodness of the model can be seen in Fig. SM5, where a comparison between measured and modeled dissolved Cl concentrations is displayed, with all samples aligned within the theoretical conservative mixing line. The comparison between the measured dissolved concentrations and those estimated based on a conservative behavior allows quantifying the removal or release rates during the suspended particles-column water interactions. As can be seen in Fig. SM6, there exists a net Tl release in the Tinto estuary from suspended particulate matter during the DS (from 144 to 586% of expected concentrations), especially high in the low to medium salinity range (10–39% of seawater contribution). On the other hand, removal rates ranging from 54 to 70% in the Tinto estuary were observed during the WS, with no apparent pattern related to salinity. These differences may be related to the sharp and quick (from minutes to hours) hydrochemical changes, especially for trace metals, of the Tinto River during flood events (Cánovas et al., 2021), making unsuitable as end-member in the mixing model.

In the case of the Odiel estuary, a progressive release of Tl is observed during the DS (from 31 to 541%) associated to the salinity increase (from 10 to 94% of seawater contribution). A similar pattern is observed during the WS, with slight removal rates (up to 8%) in the low salinity zone (<1% of seawater contribution) and progressive release rates (from 22 to 208%) with increasing salinity (from 10 to 65% of seawater contribution). The mixing model suggest higher Tl release from suspended particulate matter in the lower reaches of the Odiel estuary, when dilution seems to be the dominant factor (Fig. SM6). Therefore, this Tl release may be not directly observable in the decreasing bulk concentrations of dissolved Tl with predominance of seawater influence as they are hampered by the dilution effect due to the huge amounts of seawater mixed with river water.

3.5. Impact of mine spills on the transfer of Tl to the oceans

Accidental mining spills may lead to increasing metal concentrations and loadings to the oceans in mineralized watersheds. This is the case of the Odiel watershed, where around 270,000 m^3 of AMD waters were spilled in May 2017 after the collapse of a concrete plug of an old adit connected to La Zarza pit lake (Olías et al., 2019). In the case of Tl, dissolved concentrations reached during the spill (May 2017) were slightly higher both in the Odiel estuary (from 0.55 to 0.23 μg/L) and the channel (from 0.23 to 0.03 μg/L) than during a similar period (DS, May 2018; Table 1). Comparing the dissolved Tl concentrations measured in the estuary with estimated values based on a conservative mixing model, dissolved Tl concentrations measured were higher than expected. The intense precipitation of Fe in the river after the spill caused the occurrence of abundant Fe suspended colloids in the water column, which may host significant amounts of trace metals such as As or Tl. Therefore, the interaction of these Fe colloids with seawater may have released back these metal/loids to the water column. This transference of Tl from suspended particles to the water column can be quantified considering the end-members' (*i.e.*, river and seawater) contribution. Thus, a moderate increase in dissolved Tl concentrations was observed in the low-medium salinity zone (<50% of Tl release below 50% seawater contribution) whereas an enhanced release was observed at the high salinity zone (up to around 1100% of Tl release; Fig. SM7). These values are more than double than those observed for the same period (DS) the following year (Fig. SM6), highlighting the impact of the mine spill on the remobilization of Tl from the suspended particulate matter to the water column.

4. Conclusions

This study investigates the mobility of Tl in the Ría de Huelva (SW Spain), one of the most metal polluted estuaries in the world, by collecting water samples and suspended particles in several estuarine transects during different hydrological regimes. In the Tinto and Odiel rivers, Tl is released due to sulfide oxidation (where Tl can be found as impurity) in mining areas and the dissolution of host rock minerals due to extreme acidity during sulfide oxidation. Tl is transported downstream from mining areas by the Tinto and Odiel rivers, where suffers from coprecipitation/adsorption processes onto Fe minerals (i.e., mainly jarosite), to the estuary. Tl concentration displayed a general decrease across the estuary; from 5.0 to 0.34 μg/L in the Tinto and Odiel estuaries, respectively, to 0.02 μg/L in the channel during the DS, being more attenuated during the WS (from 0.72 to 0.14 μg/L in the Tinto and Odiel estuaries, respectively, to 0.02 μg/L in the channel) due to the dilution effect of rainfalls in the watersheds. However, different increases in Tl concentrations with salinity were observed in the upper reaches of the Tinto and Odiel estuaries during the dry and wet season, respectively.

Examination of suspended particulate by SEM-EDX revealed the presence of Fe (hydr)oxysulfate phases in the Tinto estuary with a chemical composition similar to jarosite and schwertmannite, and Al hydroxysulfate, coating other minerals, including Fe (hydr)oxysulfate, in the Odiel estuary. The solid concentrations of Tl exhibited a good positive correlation with Fe ($R^2 = 0.86$) and As ($R^2 = 0.81$) and negative correlation with Al ($R^2 = 0.87$). Poorer correlations were observed between Tl and other elements, such as Mn, Si, or K, suggesting that particulate Tl transport in the estuary is exclusively driven by Fe minerals. The increase in Tl concentration with salinity observed in the estuary, especially in the low salinity zone, may be related to the desorption of Tl^+ from jarosite during the mixing of river with seawater. Thus, Tl may be released back from jarositic in suspended particulate matter across the salinity gradient due to the increasing proportion of unreactive $TlCl^0$ and K^+ ions, which compete for adsorption sites with Tl^+ at increasing salinity. A mixing model based on conservative elements allowed quantifying this release with respect to conservative concentrations (up to 586%).

A mining spill occurred in the Odiel watershed in May 2017 led to increasing concentrations of dissolved and particulate Tl in the estuary, enhancing these desorption processes observed in the estuary highlighting the impact of the mine spill on the remobilization of Tl from the suspended particulate matter to the water column.

Credit author statement

C.R. Cánovas: Conceptualization, Funding acquisition, Writing - Original Draft, Visualization, Writing - Review & Editing,; **M. D Basallote:** Methodology, Investigation, Writing - Review & Editing; **F. Macías:** Formal Analysis, Validation, Writing - Review & Editing; **R. Freydier:** Conceptualization, Investigation, Supervision, Writing - Review & Editing; **A.Parviainen**: Methodology, Investigation, Writing - Review & Editing; **R. Pérez-López**: Project administration, Funding acquisition, Supervision, Writing - Review & Editing.

Declaration of competing interest

The authors declare that they have no known competing financial interests or personal relationships that could have appeared to influence

the work reported in this paper.

Acknowledgments

This work was supported by the Spanish Ministry of Economy and Competitiveness under the research projects CAPOTE (MINECO; CGL 2017-86050-R) and TRAMPA (MINECO; PID 2020-119196RB-C21). C.R Cánovas thanks the Spanish Ministry of Science and Innovation for the Postdoctoral Fellowship granted under application reference RYC 2019-027949-I. M.D. Basallote thanks the Spanish Ministry of Science and Innovation for the Postdoctoral Fellowship granted under application reference IJC 2018-035056-I. A. Parviainen thanks the Spanish Ministry of Science and Innovation for the Postdoctoral Fellowship granted under application reference IJCI-2016-27412. The comments and helpful criticisms of three anonymous reviewers and the support of Professor Wen-Xiong Wang (Editor) have considerably improved the original manuscript and are also gratefully acknowledged. Funding for open access charge: Universidad de Huelva/CBUA.

Appendix A. Supplementary data

Supplementary data to this article can be found online at https://doi.org/10.1016/j.envpol.2022.119448.

References

Acero, P., Ayora, C., Torrento, C., Nieto, J.M., 2006. The behavior of trace elements during schwertmannite precipitation and subsequent transformation into goethite and jarosite. Geochem. Cosmochim. Acta 70, 4130–4139. https://doi.org/10.1016/j.gca.2006.06.1367.

Aguilar-Carrillo, J., Herrera-García, L., Reyes-Domínguez, I.A., Gutiérrez, E.J., 2020. Thallium (I) sequestration by jarosite and birnessite: structural incorporation vs surface adsorption. Environ. Pollut. 257, 113492. https://doi.org/10.1016/j.envpol.2019.113492.

Allison, J.D., Brown, D.S., Novo-Gradac, J., 1999. MINTEQA2/PRODEAFA2, a Geochemical Assessment Model for Environmental Systems: User Manual Supplement for Version 4.0. US EPA, NERL, Athens, Georgia.

Anagboso, M.U., Turner, A., Braungardt, C., 2013. Fractionation of thallium in the Tamar estuary, south west England. J. Geochem. Explor. 125, 1–7. https://doi.org/10.1016/j.gexplo.2012.10.018.

Asta, M.P., MLl, Calleja, Pérez-López, R., Auqué, L.F., 2015. Major hydrogeochemical processes in an acid mine drainage affected estuary. Mar. Pollut. Bull. 91, 295–305. https://doi.org/10.1016/j.marpolbul.2014.11.023.

Belzile, N., Chen, Y.W., 2017. Thallium in the environment: a critical review focused on natural waters, soils, sediments and airborne particles. Appl. Geochem. 84, 218–243. https://doi.org/10.1016/j.apgeochem.2017.06.013.

Böning, P., Ehlert, C., Niggemann, J., Schnetger, B., Pahnke, K., 2017. Thallium dynamics in the Weser estuary (NW Germany). Estuar. Coast Shelf Sci. 187, 146–151. https://doi.org/10.1016/j.ecss.2016.12.004.

Campanella, B., Colombaioni, L., Benedetti, E., Di Ciaula, A., Ghezzi, L., Onor, M., D'Orazio, M., Giannecchini, R., Petrini, R., Bramanti, E., 2019. Toxicity of thallium at low doses: a review. Int. J. Environ. Res. Publ. Health 16, 4732. https://doi.org/10.3390/ijerph16234732.

Cánovas, C.R., Olias, M., Nieto, J.M., Sarmiento, A.M., Cerón, J.C., 2007. Hydrogeochemical characteristics of the Odiel and Tinto rivers (SW Spain). Factors controlling metal contents. Sci. Total Environ. 373, 363–382. https://doi.org/10.1016/j.scitotenv.2006.11.022.

Cánovas, C.R., Basallote, M.D., Macias, F., 2020a. Distribution and availability of rare earth elements and trace elements in the estuarine waters of the Ría of Huelva (SW Spain). Environ. Pollut. 267, 115506. https://doi.org/10.1016/j.envpol.2020.115506.

Cánovas, C.R., Basallote, M.D., Borrego, P., Millán-Becerro, R., Pérez-López, R., 2020b. Metal partitioning and speciation in a mining-impacted estuary by traditional and passive sampling methods. Sci. Total Environ. 722, 137905. https://doi.org/10.1016/j.scitotenv.2020.137905.

Cánovas, C.R., Basallote, M.D., Macías, F., Olías, M., Pérez-López, R., Ayora, C., Nieto, J. M., 2021. Geochemical behaviour and transport of technology critical metals (TCMs) by the Tinto River (SW Spain) to the Atlantic Ocean. Sci. Total Environ. 764, 143796. https://doi.org/10.1016/j.scitotenv.2020.143796.

Carrera, J., Vázquez-Suñé, E., Castillo, O., Sánchez-Vila, X., 2004. A methodology to compute mixing ratios with uncertain end-members. Water Resour. Res. 40, W12101. https://doi.org/10.1029/2003WR002263.

Carro, B., Borrego, J., Morales, J.A., 2018. Estuaries of the huelva Coast: Odiel and Tinto estuaries (SW Spain). In: Morales, J. (Ed.), The Spanish Coastal Systems. Springer, Cham, Springer Nature Switzerland. https://doi.org/10.1007/978-3-319-93169-2_23.

Casiot, C., Egal, M., Bruneel, O., Verma, N., Parmentier, M., Elbaz-Poulichet, F., 2011. Predominance of aqueous Tl(I) species in the river system downstream from the abandoned Carnoules Mine (Southern France). Environ. Sci. Technol. 45, 2056–2064. https://doi.org/10.1021/es102064r.

Coup, K.M., Swedlund, P.J., 2015. Demystifying the interfacial aquatic geochemistry of thallium(I): new and old data reveal just a regular cation. Chem. Geol. 398, 97–103. https://doi.org/10.1016/j.chemgeo.2015.02.003.

Dutrizac, J.E., Chen, T.T., Beauchemin, S., 2005. The behaviour of thallium(III) during jarosite precipitation. Hydrometallurgy 79, 138–153. https://doi.org/10.1016/j.hydromet.2005.06.003.

Elbaz-Poulichet, F., Morley, N.H., Beckers, J.M., Nomerange, P., 2001. Metal fluxes through the strait of Gibraltar: the influence of the Tinto and Odiel rivers (SW Spain). Mar. Chem. 73, 193–213. https://doi.org/10.1016/S0304-4203(00)00106-7.

European Commission, 2000. Directive 2000/60/EC of the European Parliament and the Council of 23.10.2000. A framework for community action in the field of water policy. Off. J. Eur. 72. Communities 22.12.2000.

Jacobson, A.R., McBride, M.B., Baveye, P., Steenhuis, T.S., 2005. Environmental factors determining the trace-level sorption of silver and thallium to soils. Sci. Total Environ. 345, 191–205. https://doi.org/10.1016/j.scitotenv.2004.10.027.

Law, S., Turner, A., 2011. Thallium in the hydrosphere of south west England. Environ. Pollut. 159, 3484–3489. https://doi.org/10.1016/j.envpol.2011.08.029.

Lecomte, K.L., Sarmiento, A.M., Borrego, J., Nieto, J.M., 2017. Rare earth elements mobility processes in an AMD-affected estuary: huelva Estuary (SW Spain). J. Mar. Pollut. Bull. 121, 282–291. https://doi.org/10.1016/j.marpolbul.2017.06.030.

Lin, T.S., Nriagu, J.O., 1998. Speciation of Thallium in Natural Waters. In: Nriagu, J.O. (Ed.), Thallium in the Environment, Advances in Environmental Sci. and Technology, Vol. 29. Wiley and Sons, NY, pp. 31–44.

Lis, J., Pasieczna, A., Karbowska, B., Zembrzuski, W., Lukaszewski, Z., 2003. Thallium in soils and stream sediments of a Zn-Pb mining and smelting area. Environ. Sci. Technol. 37, 4569–4572. https://doi.org/10.1021/es0346936.

Liu, J., Yin, M., Xiao, T., Zhang, C., Tsang, D., Bao, Z., Zhou, Y., Chen, Y., Luo, X., Yuan, W., Wang, J., 2020. Thallium isotopic fractionation in industrial process of pyrite smelting and environmental implications. J. Hazard Mater. 384, 121378. https://doi.org/10.1016/j.jhazmat.2019.121378.

Martín-Ramos, J.D., 2004. Using XPowder: a Software Package for Powder X-Ray Diffraction Analysis, D.L. GR-1001/04 84-609-1497-6. Spain. http://www.xpowder.com.

Nielsen, S.G., Rehkämper, M., Porcelli, D., Andersson, P., Halliday, A.N., Swarzenski, P. W., Latkoczy, C., Gunther, D., 2005. Thallium isotope composition of the upper continental crust and rivers - an investigation of the continental sources of dissolved marine thallium. Geochem. Cosmochim. Acta 69, 2007–2019. https://doi.org/10.1016/j.gca.2004.10.025.

Nieto, J.M., Sarmiento, A.M., Cánovas, C.R., Olías, M., Ayora, C., 2013. Acid mine drainage in the Iberian Pyrite Belt: 1. Hydrochemical characteristics and pollutant load of the Tinto and Odiel rivers. Environ. Sci. Pollut. Res. 20, 7509–7519. https://doi.org/10.1007/s11356-013-1634-9.

NIST, 2004. In: Martell, A.E., Smith, R.M. (Eds.), NIST Standard Reference Database. Gaithersburg, USA.

Nordstrom, D.K., Wilde, F.D., 1998. Reduction-oxidation potential (electrode method), Section 6.5, Chapter A6. National Field Manual for the Collection of Water-Quality Data, p. 20.

Nuvolone, D., Petri, D., Aprea, M.C., Bertelloni, S., Voller, F., Aragona, I., 2021. Thallium contamination of drinking water: health implications in a residential Cohort study in Tuscany (Italy). Int. J. Environ. Res. Publ. Health 18, 4058. https://doi.org/10.3390/ijerph18084058.

Olías, M., Cánovas, C.R., Basallote, M.D., Macías, F., Pérez-López, R., Moreno González, R., Millán-Becerro, R., Nieto, J.M., 2019. Causes and impacts of a mine water spill from an acidic pit lake (Iberian Pyrite Belt). Environ. Pollut. 250, 127–136. https://doi.org/10.1016/j.envpol.2019.04.011.

Ridderinkhof, H., van der Ham, R., van der Lee, W., 2000. Temporal variations in concentration and transport of suspended sediments in a channel-flat system in the Ems-Dollard Estuary. Continent. Shelf Res. 20, 1479–1493.

Sibrell, P., Montgomery, G., Ritenour, K., Tucker, T., 2009. Removal of phosphorus from agricultural wastewaters using adsorption media prepared from acid mine drainage sludge. Water Res. 43, 2240–2250. https://doi.org/10.1016/j.watres.2009.02.010.

Tremel, A., Masson, P., Sterckeman, T., Baize, D., Mench, M., 1997. Thallium in French agrosystems—I. Thallium contents in arable soils. Environ. Pollut. 95, 293–302. https://doi.org/10.1016/S0269-7491(96)00145-5.

Turner, A., Millward, G.E., 2002. Suspended particles: their role in estuarine biogeochemical cycles. Estuar. Coast Shelf Sci. 55, 857–883. https://doi.org/10.1006/ecss.2002.1033.

Turner, A., 1996. Trace-metal partitioning in estuaries: importance of salinity and particle concentration. Mar. Chem. 54, 27–39. https://doi.org/10.1016/0304-4203(96)00025-4.

Turner, A., Cabon, A., Glegg, G.A., Fisher, A.S., 2010. Sediment-water interactions of thallium under simulated estuarine conditions. Geochem. Cosmochim. Acta 74, 6779–6787. https://doi.org/10.1016/j.gca.2010.09.004.

USEPA, 2014. United States Environmental Protection Agency. Office of Science and Technology. National Recommended Water Quality Criteria - Human Health Criteria. https://www.epa.gov/wqc/national-recommended-water-quality-criteria-human-health-criteria-table.

USEPA, 2015. Unites States Environmental Protection Agency. Toxic and Priority Pollutants under the Clean Water Act. https://www.epa.gov/eg/toxic-and-priority-pollutants-under-clean-water-act.

Verweij, W., 2017. Manual for CHEAQS Next, a Program for Calculating Chemical Equilibria in Aquatic Systems.

Vink, B.W., 1993. The behavior of thallium in the (sub)surface environment in terms of Eh and pH. Chem. Geol. 109, 119–123. https://doi.org/10.1016/0009-2541(93)90065-Q.

Wang, J., She, J., Zhou, Y., Tsang, D., Beiyuan, J., Xiao, T., Dong, X., Chen, Y., Liu, J., Yin, M., Wang, L., 2020. Microbial insights into the biogeochemical features of thallium occurrence: a case study from polluted river sediments. Sci. Total Environ. 739, 139957. https://doi.org/10.1016/j.scitotenv.2020.139957.

Webster, I.T., Hancock, G.J., Murray, A.S., 1995. Modelling the effect of salinity on radium desorption from sediments. Geochem. Cosmochim. Acta 59, 2469–2476.

Wick, S., Peña, J., Voegelin, A., 2019. Thallium sorption onto manganese oxides. Environ. Sci. Technol. 53 (22), 13168–13178. https://doi.org/10.1021/acs.est.9b04454.

Yin, M., Zhou, Y., Tsang, D., Beiyuan, J., Song, L., She, J., Wang, J., Zhu, L., Fang, F., Wang, L., Liu, J., Liu, Y., Song, G., Chen, D., Xiao, T., 2021. Emergent thallium exposure from uranium mill tailings. J. Hazard Mater. 407, 124402. https://doi.org/10.1016/j.jhazmat.2020.124402.

Yu, J.Y., Heo, B., Choi, I.K., Cho, J.P., Chang, H.W., 1999. Apparent solubilities of schwertmannite and ferrydrite in natural stream waters polluted by mine drainage. Geochem. Cosmochim. Acta 63, 3407–3416.